

Automated Planning for Multi-Objective Machine Tool Calibration: Optimising Makespan and Measurement Uncertainty

**Simon Parkinson, Andrew P. Longstaff
Andrew Crampton**

Centre for Precision Technologies
School of Computing and Engineering
University of Huddersfield, UK
s.parkinson@hud.ac.uk
a.p.longstaff@hud.ac.uk

Peter Gregory

Digital Futures Institute
School of Computing
Teesside University, UK
p.gregory@tees.ac.uk

Abstract

The evolution in precision manufacturing has resulted in the requirement to produce and maintain more accurate machine tools. This new requirement coupled with desire to reduce machine tool downtime places emphasis on the calibration procedure during which the machine's capabilities are assessed. Machine tool downtime is significant for manufacturers because the machine will be unavailable for manufacturing use, therefore wasting the manufacturer's time and potentially increasing lead-times for clients. In addition to machine tool downtime, the uncertainty of measurement, due to the schedule of the calibration plan, has significant implications on tolerance conformance, resulting in an increased possibility of false acceptance and rejection of machined parts.

The work presented in this paper is focussed on expanding a developed temporal optimisation model to reduce the uncertainty of measurement. Encoding the knowledge in regular PDDL requires the discretization of non-linear, continuous temperature change and implementing the square root function. The implementation shows that not only can domain-independent automated planning reduce machine downtime by 10.6% and the uncertainty of measurement by 59%, it is also possible to optimise both metrics reaching a compromise that is on average 9% worse than the best-known solution for each individual metric.

Introduction

Machine tools are mechanically powered devices used during subtractive manufacturing to cut material. The design and configuration of a machine tool is chosen for a particular role and is different depending on the volume and complexity range of work-pieces. A common factor throughout all configurations of machine tools is that they provide the mechanism to support and manoeuvre their axes around the work-piece. The physical manner by which the machine moves is determined by the machine's kinematic chain. The kinematic chain will typically constitute a combination of linear and rotary axes. For example, Figure 1 illustrates a three-axis machine tool consisting of three linear axes.

In a perfect world, a machine tool would be able to move to predictable points in three-dimensional space, resulting in a machined artefact that is geometrically identical to the designed part. However, due to tolerances in the production of

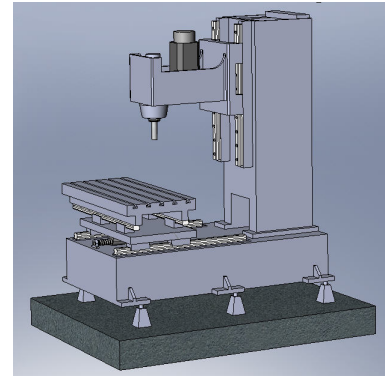


Figure 1: Example three-axis machine tool

machine tools, this is very difficult to achieve. For example, Figure 2 shows the pseudo-static errors (those resulting from the movement of the machine tool's axes) of an axis of linear motion.

Machine tool calibration is the process of assessing a machine tool's manufacturing capabilities that includes error classification, measurement and analysis (Schwenke *et al.* 2008). Performing a machine tool calibration contributes to the machine's accuracy by providing detailed analysis of the machine's geometric capabilities which can subsequently be used to determine corrective action, and provide confidence that a given asset is capable of machining a part within a predefined tolerance. At present, there is no standard way to plan a machine tool calibration and plans can be created *ad hoc* or in the order they were done previously. Planning is required because there are multiple different ways of measuring the same error, and the most suitable selection is not known in advance. This is problematic because machine tool manufacturers and users require that machine tool downtime is minimised due to the associated financial implications (Shagluf, Longstaff, & Fletcher 2013). However, currently there is little consideration taken by those planning machine tool calibrations to reduce machine tool downtime.

In addition to costs associated with downtime, it is also important for companies to produce and maintain more accurate machine tools. Each measurement taken during calibration has an associated uncertainty of measurement. The

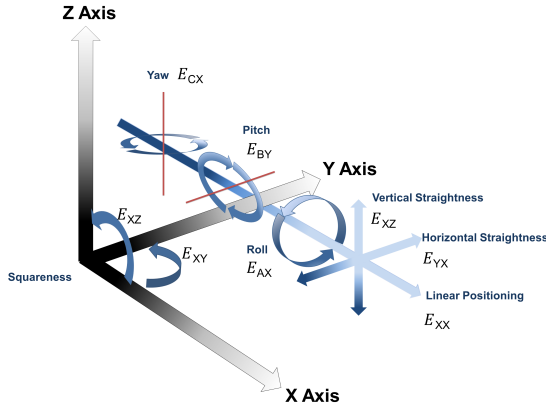


Figure 2: Linear motion errors

uncertainty of measurement can be regarded as the doubt that exists about the result of any measurement and confidence in this assessment (Bell 2001; Birch 2003).

For example, measuring length using a ruler might result in an uncertainty of ± 1 mm. Therefore, it can be stated that when the result of a measurement is 20 mm, it is actually $20 \text{ mm} \pm 1 \text{ mm}$ with a confidence level of 95%. Quantifying and reducing measurement uncertainty is an important task in that it is required to be reported on the calibration certificate.

In this work, we describe a multi-objective planning model in which both the makespan and measurement uncertainty are taken into consideration. We consider both the uncertainty due to individual measurements and also the uncertainty due to interacting measurements. This requires reasoning about the environmental temperature in which the machine operates. Further, we show that there is a compromise between optimising measurement uncertainty and optimising the makespan of the plan; plans that minimise makespan do not necessarily have low measurement uncertainty, and vice versa. We provide evidence that good quality solutions can be found in which both metrics are around ten percent lower in quality than the best found solutions for the individual metrics.

The next section in this paper describes previous work into machine tool downtime reduction, providing sufficient detail for the reader to understand the extensions made in the multi-objective model. Following this, a detailed description of the extension of the temporal domain to model the necessary factors to reduce the uncertainty of measurement due to the order of the plan is provided. Equations for estimating the uncertainty of measurement when using a laser interferometer are provided as an example. Next, experimental analysis is provided showing how the model performs when optimising for time and uncertainty of measurement separately and then in unison. Following this, excerpts from industrial plans are shown to illustrate the ability to reduce machine tool downtime and the uncertainty of measurement separately and then together. The paper then concludes by highlighting the success of the implementation and laying

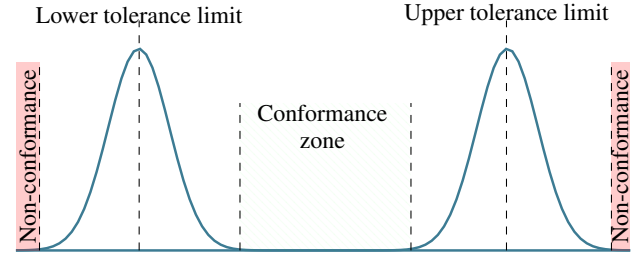


Figure 3: Conformance and non-conformance zones for two-sided tolerance. A valid measurement must lie between the lower and upper tolerance limits. However, due to measurement uncertainty, measurements close to the tolerance limits on either side cannot be guaranteed to be correctly classified.

out scope for future work.

Importance of Reducing Measurement Uncertainty

The uncertainty of measurement is dependent on many factors such as the measurement instrumentation, method of measurement, and the propagation of interrelated geometric errors. One of the main factors to influence a measurement's uncertainty is the change in environmental temperature. In addition, the uncertainty of measurement can propagate through to interrelated measurements, thus the order that the measurements are measured in can significantly affect the combined uncertainty of measurement.

The requirement to reduce the estimated uncertainty of measurement is because of its effect on tolerance conformance (i.e. our ability to say with certainty that a measurement lies within a particular interval). Figure 3 illustrates the conformance (green) and non-conformance (red) zones based on the uncertainty value and the lower and upper tolerance limit (Forbes 2006; BIPM 2008). The remainder is uncertain: the curves in Figure 3 show the likelihood that a given measurement is incorrect.

The term *false acceptance* refers to when a machined part incorrectly passes quality control checks. The term *false rejection* refers to when an adequately machined part is incorrectly rejected because of an incorrect assessment. Figure 3 illustrates the effect that the uncertainty of measurement has on false acceptance and rejection. False acceptance occurs when the measurement value is out-of-tolerance but the uncertainty of measurement brings it into tolerance. Conversely, false rejection occurs when the measured value is in tolerance but the uncertainty of the measurement makes it out-of-tolerance. Therefore, only measurement values that fall within the conformance zone are certain, within the given confidence level, to be within the tolerance. Minimising the uncertainty of measurement can increase the size of the conformance zone, thus reducing false acceptance and rejection.

For example, using the example of a ruler, if a length was required to be $20 \text{ mm} \pm 2 \text{ mm}$, it would only conform if the real length was between 18.1 mm and 21.9 mm. This is

because the ruler has a 0.1 mm uncertainty. Likewise, if the uncertainty were ± 0.5 mm, the reading will only conform if it is between 18.5 mm and 21.5 mm. Therefore, a tolerance of ± 2 mm is reduced to conformance of ± 1.5 mm.

Although the uncertainty of measurement must be recorded on calibration certificates, there is an absence of literature suggesting that the uncertainty of measurement due to the whole calibration plan (sequence of measurements) is being considered, either by manual or automated techniques.

One reason for this is that the complexities involved with scheduling each measurement to minimize their effect on the cumulative uncertainty of measurement is a difficult task that requires detailed knowledge of the machine and the measuring instrumentation. Another reason is that creating a calibration plan that reduces measurement uncertainty may increase the time required for calibration, thus costing the machine tool owner time and money in the short term.

Temporal Optimisation Model

In previous work, a PDDL2.2 domain model was produced modelling the process of machine tool calibration planning and allowing for the construction of temporally optimal calibration plans (Parkinson *et al.* 2012b). The PDDL2.2 temporal optimisation model consists of the following durative actions:

Set-up: Setting up of an instrument to measure a specific error component on a specific axis.

Measure: The measurement procedure is where the error is examined.

Remove: Removing the instrument from the current set-up.

Adjust Error: Adjusting the instrument to measure a different error.

Adjust Position: Sometimes the instrument cannot measure the entire axis at once, so it is necessary to break the measurement up into small measurements.

The model's ability to produce machine tool calibration plans that are temporally optimised has been empirically validated by performing industrial case-studies (Parkinson *et al.* 2012a). In these case-studies, the LPG-td (Gerevini, Saetti, & Serina 2008) planner was used because of its competitive performance (Long & Fox 2003) and its support for PDDL2.2, ADL, and Timed Initial Literals (Gerevini, Saetti, & Serina 2006). When compared to the current state-of-the-art in machine tool calibration planning, the PDDL model could produce calibration plans that on average result in a 10.6% reduction in machine tool downtime. Based on industrial experience, this equates to a £134 for a single machine tool, and a £2680 for a machine shop with twenty machine tools.

Uncertainty Estimation

ISO 230 part 1 (ISO230 2012) defines linear deviation as "...the straightness of the trajectory of the functional point or the representative point of a moving component." In this work, the measurement of linear deviation (positioning) using a laser interferometer is considered. The following

section provides the equations for estimating uncertainty of measurement as found in (ISO 230-9 2005).

Firstly, the device's calibration certificate is used to calculate its uncertainty (u_D) using Equation 1 where the calibration uncertainty ($U_{CALIBRATION}$) has been provided in micrometers per metre ($\mu\text{m}/\text{m}$). If the calibration uncertainty is provided in micrometers (μm) the length L should be removed.

$$u_D = \frac{U_{CALIBRATION} \times L}{k} \quad (1)$$

Measuring positioning error using laser interferometry requires the alignment of the laser beam parallel to the axis under test. A misalignment between the laser and axis can be observed and can be reduced by manual adjustment of the laser. Misalignment of the laser has a second order effect on the measurement and the difference in length (ΔL_M) as a result of the misalignment can be calculated using Equation 2. However, the misalignment for many devices, such as laser interferometers, have a misalignment within ± 1 mm. Therefore, in this paper we define ΔL_M to 1.

$$\Delta L_M = L \times (1 - \cos \gamma) \times 1000 \quad (2)$$

The influence of the misalignment can be significant on short travel axes. From the difference in length, the uncertainty contribution (u_M) can then be calculated using Equation 3.

$$u_M = \frac{\Delta L_M}{2\sqrt{3}} \quad (3)$$

As stated in ISO 230 part 2 (ISO 230-2 2006) in Section 3.1, the "measuring instrument and the measured object are soaked in an environment at a temperature of 20°C " before any measurement takes place. Therefore, any deviation from this temperature should result in compensation of the machine tool. This compensation introduces the uncertainty of the temperature measurement, and the uncertainty of the coefficient of thermal expansion of the machine tool. Equation 4 provides the method for calculating the uncertainty due to the temperature change of the machine tool ($u_{M,M}$). Equation 5 describes how to calculate the uncertainty due to the coefficient of thermal expansion of the machine tool ($u_{E,M}$). Where α is the coefficient of thermal expansion of the machine tool in μm , $R(\theta)$ is the possible range due to uncertainty of the temperature difference of the machine tool and the measuring device in $^\circ\text{C}$, $R(\alpha)$ is the error range of expansion coefficient of machine tool in $\mu\text{m}/(\text{m}^\circ\text{C})$, and $T\Delta$ is the difference to 20°C in degrees Celsius, $T\Delta = T - 20^\circ\text{C}$.

$$u_{M,M} = \alpha \times L \times R(\theta) \quad (4)$$

$$u_{E,M} = T\Delta \times L \times R(\alpha) \quad (5)$$

Similarly to the machine tool, the measurement device uncertainty ($u_{M,D}$) will also need to be compensated due to the temperature, as well as the uncertainty due to the coefficient of thermal expansion ($u_{E,D}$). Equation 6 describes

how to calculate the device uncertainty due to the temperature measurement, and Equation 7 shows how to calculate the uncertainty due to the coefficient of thermal expansion of the device. In some cases, such as when using a laser interferometer, the device will automatically compensate for temperature change of the device and machine tool using environmental monitoring. In this particular example it is not necessary to calculate $u_{M,D}$ and $u_{E,D}$ as they are automatically compensated for by the device. However, it is worth noting that the compensation will have uncertainty, and consideration should be taken to include this uncertainty, no matter how small.

$$u_{M,D} = \alpha \times L \times R(\theta) \quad (6)$$

$$u_{E,D} = T\Delta \times L \times R(\alpha) \quad (7)$$

During measurement, the temperature of the environment might change resulting in the possibility of instrument and machine tool drift that influences the measurement result. An experiment can be performed to monitor drift by leaving the instrument active for a period of time equal to the length of time for the test to identify any change in the value relative to temperature. From this, Equation 8 can be used to determine the uncertainty due to environmental variation u_{EVE} . A downside of this approach is that it doubles the length of time to perform the measurement.

$$u_{EVE} = \frac{E_{VE}}{2\sqrt{3}} \quad (8)$$

Equation 9 shows the calculation necessary to compute the estimated uncertainty for one measurement (BIPM 2008). However, many measurements will be made when calibrating a machine tool, making the combined uncertainty u the sum of all u_c .

$$u_c = \sqrt{u_D^2 + u_M^2 + u_{M,M}^2 + u_{M,D}^2 + u_{E,M}^2 + u_{E,D}^2 + u_{EVE}^2} \quad (9)$$

When considering interrelated measurements, individual errors can significantly increase the error of interrelated measurements. For example, the squareness error of two perpendicular axes is calculated using the straightness of the two axes. Therefore, any increase in their measurement error would also increase the measurement error in the squareness.

When interrelated errors, u_{ERR_i} , are to be included, Equation 9 is expanded to include them. Where u_{ERR_i} is the maximum permissible interrelated error value or is to be calculated once their uncertainties are known. The model presented in this paper considers instances where two interrelated errors u_{ERR_1} and u_{ERR_2} are included in a measurement's uncertainty estimation. However, this can easily be expanded to include the propagation of uncertainty from many different sources.

The expanded uncertainty U can then be calculated by using Equation 10 where the combined standard uncertainty is multiplied by the coverage factor k .

$$U = k \times u_c \quad (10)$$

Uncertainty of Measurement Optimisation Model

For this investigation, conditions that affect the uncertainty irrespective of the plan are ignored. This means that it is only necessary to model aspects that cause the estimated uncertainty of measurement to change, thus simplifying the numerical aspects of the domain model.

Factors That Affect The Uncertainty of Measurement

There are many potential contributors that affect the uncertainty of measurement. However, when automatically constructing a calibration plan, the aim is to select the most suitable instrumentation and measurement technique that has the lowest estimated uncertainty. In addition, the estimated uncertainty should take into consideration the changing environmental data, and where possible, schedule the measurements to take place where the effect of temperature on the estimated uncertainty is at its lowest.

The following list provides the factors that affect the estimated uncertainty of the calibration plan, and suggests how they can be optimised

- Measurement instrumentation with the lowest estimated uncertainty of measurement (u_D). Where possible, intelligently selecting instrumentation with the lowest uncertainty will reduce the overall estimated uncertainty of measurement.
- The change in environmental temperature throughout the duration of a measurement can significantly increase the uncertainty of measurement. When possible, the measurement should be scheduled to take place where the temperature is stable (u_{EVE}).
- When considering interrelated measurements, the change in environmental temperature between their measurement can significantly increase the uncertainty. For example, the squareness error of two perpendicular axes is calculated using the straightness of the two axes. Therefore, any temperature change throughout and between their measurement would increase the squareness' estimated uncertainty of measurement. During planning, it is important to schedule interrelated measurements where the change in environmental temperature is minimum.

Domain Modelling

The previously developed temporal model (Parkinson *et al.* 2012b) is extended to encode the knowledge of uncertainty of measurement reduction. Figure 4 shows the functional flow between the PDDL actions within the new model. In the figure, durative actions are represented using a circle with a solid line. Figure 4 shows that the measurement action has been split up into two different actions. In addition there is an adjust action which may need to be executed if the instrumentation is not effective for the travel length of

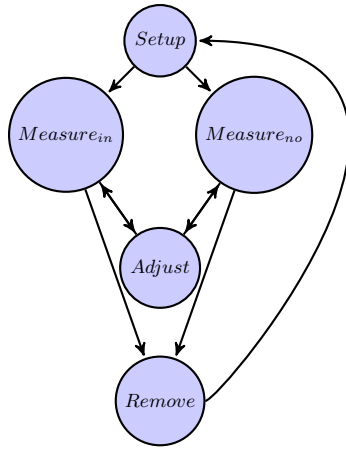


Figure 4: Illustration showing the PDDL actions and their functional flow.

the axis. It is necessary to have two versions of the measurement action because not all measurements have other errors propagating down the kinematic chain and effecting their uncertainty. The following list details the extension of the measurement action into two actions along with and adjustment action:

Measure_{no} : The measurement action represents a measurement where no consideration is required to be taken for any influencing errors.

Measure_{in} : Conversely, this measurement action represents a measurement where consideration is required to be taken because of influencing errors.

Adjust : Some axes are longer than the range of the measuring device. In this case, the measuring device needs to readjusted several times in order to measure the full range of the axis.

The developed model is encoded in PDDL 2.1. This is because we use numbers, time, and durative actions (Fox & Long 2003). We use regular numeric fluents to model constants and variables relating to the uncertainty of measurements. For example, a device's uncertainty ($U_{DEVICE\ LASER}$) can be represented in PDDL as $(=(device-u\ ?i - instrument)0.001)$ where the instrument object $?i$ has the value of $0.001\ \mu m$.

In the temporal model, the cost of each action is the time taken to perform that specific task. Using this model will produce a calibration plan, indicating the ordering of the measurements and the time taken to perform each test. In order to encode Equations 5 and 7, we need the access to the change in environmental temperature ($T\Delta$ in the equations) that occurs between the the start and end of a measurement. Assuming we have access to the temperature as a fluent (this will be discussed later), we can sample the value at the start and end of the measurement with the `at start` and `at end` syntax of PDDL. Thus, we record a temporary value (`start-temp`) at the start of the action, and then calculate $T\Delta$ at the end of the action by subtracting the start temperature from the current temperature.

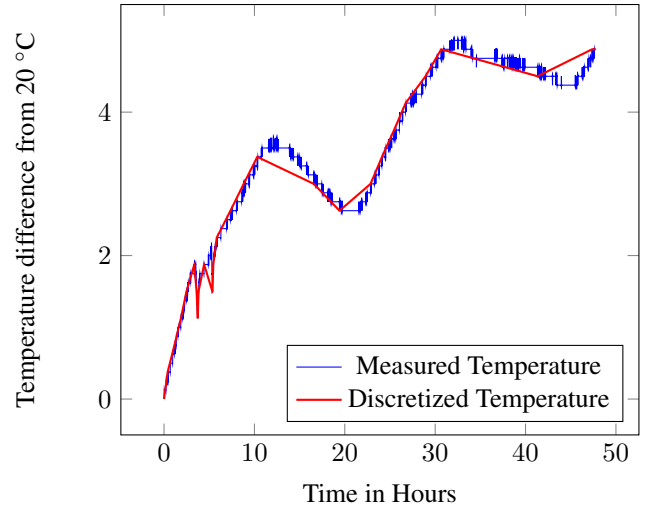


Figure 5: Graph showing both the original and discretized temperature profile. The used discretization value is 0.01

As stated previously, in order for this modelling choice to work, we need to be able to query the temperature as a fluent at any given time. The method used in order to achieve this is described in the following section.

Temperature Profile In PDDL2.1 it is not possible simply to represent predictable continuous, non-linear numeric change. More specifically, it is not possible to represent the continuous temperature change throughout the calibration process. This presents the challenge of how to optimise the sequence of measurements while considering temperature. The solution implemented in the model involves discretizing the continuous temperature change into sub-profiles of linear continuous change.

This environmental temperature profile contains the systematic heating and cooling profile for the environment of a machine tool. This information can be obtained from the machine tool owner. It is not possible to predict the non-systematic environmental temperature deviation and the magnitude of the systematic element could fluctuate slightly. However, using this systematic profile will allow us to predict how the temperature will change throughout the day, in particular where it is going to be at its lowest. Scheduling against this profile gives the best available chance of producing realistic and accurate results. During the actual calibration, deviations from the systematic profile are recorded and taken into account on the calibration certificate.

We split the continuous temperature profile into a discrete set of linear sections by iterating over the temperature data looking for a difference in temperature greater than a given sensitivity. This allows the temperature profile to be discretized into a set of linear sub-profiles. An example can be seen in Figure 5 where the environmental temperature profile (difference from $20^{\circ}C$) for a forty-eight hour period is shown (Monday and Tuesday). The chosen sensitivity, s , is based on the minimum temperature sensitivity of the available instrumentation. In this example, it is $0.1^{\circ}C$. The graph

```

(:durative-action temp-profile1
  :duration(= ?duration 42.0)
  :condition
    (and(over all(not(start0)))
      (over all (start1))))
  :effect
    (and
      (increase (temp) (*#t 0.00595))
      (at end (not(start1)))
      (at end (start2))
      (at start (clip-started))))
)

```

Figure 6: Durative actions that represents the temperature sub-profile p_1 where the duration is $t_1 = 42$.

shows the temperature profile across 48 hours; the second 24 hour period displays a higher temperature profile than the first. The reason is due to the cooling effect of the weekend where no production is taking place still being evident throughout the Monday period.

To model these sub-profiles in the PDDL model, they are represented as predetermined exogenous effects. In order to encode these in PDDL2.1, we use the standard technique of clipping durative actions together (Fox, Long, & Halsey 2004). We use the $\#t$ syntax to model the continuous linear change through the subprofile. Because the `(temp)` fluent is never used as a precondition, the measure actions can make use of the continuously changing value, without violating the *no moving targets* (Long & Fox 2003) rule. Given the predefined times t_1, \dots, t_n when the sub-profile p_1, \dots, p_n will change, a collection of durative actions, d_1, \dots, d_n are created that will occur for the durations $t_1, t_2 - t_1, \dots, t_n - t_{n-1}$. An example durative action d_1 that represents a sub-profile p_1 can be seen in Figure 6 where the duration $t_1 = 42$.

Figure 7 illustrates how the greatest deviation from 20°C (ΔT) throughout the measurement action is encoded. In this action, the temperature at the start of the measurement action, t_1 , and at the end of the action, t_2 are stored in `start-temp` and `temp` respectively. Therefore, in the measurement action it is possible to calculate the maximum temperature deviation, $T\Delta$, based on two temperatures, t_1 and t_2 .

Uncertainty Equations Implementing equations where the result is influenced by other measurements is also encoded in the PDDL using fluents. For example, Figure 8 shows the calculation for the squareness error measurement using a granite square and a dial test indicator where the uncertainty is influenced by the two straightness errors. In the model, this is encoded by assigning two fluents (`error-val ?ax ?e1`) and (`error-val ?ax ?e2`), the maximum permissible straightness error in the PDDL initial state description. This fluent will then be updated once the measurement estimation has been performed. The planner will then schedule the measurements

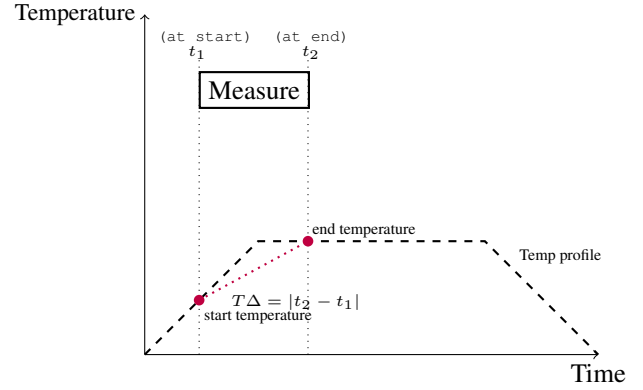


Figure 7: Illustrating showing how the current environmental temperature deviation is calculated in the measure action.

to reduce the affect that the contributing uncertainty has. Therefore, this shows how the uncertainty can be reduced due to the ordering of the plan.

When measuring an error component that does not have interrelated errors, the `measure-no-influence` action will be used which is the same as the `measure-influence` action except that it does not have the part of the equations that use the `error-val`.

Figure 8 shows the partial PDDL encoding for the estimation calculations used when performing a non-orthogonal measurement using a mechanical square and a dial test indicator. From this PDDL encoding, it is noticeable that when performing the equation to estimate $u_{E,MACHINE\ TOOL}$ (`u_t-e-c`), the temperature deviation from 20°C ($T\Delta$) supplied to the equation is the maximum deviation calculated in the PDDL action (`(- (temp) (start-temp))`).

Square Root Implementation

It is important for the planner to supply an uncertainty value in the correct units (μm) as the output from the planner will feed into a larger decision support tool and calibration engineers expect to see uncertainty reported in this way. Therefore, it was important to implement the uncertainty equations fully, including the square root function. To enable this, we modified a version of the LPG-td (Gerevini, Saetti, & Serina 2008) planner so that it parses, and plans using the `sqrt` function. Its use in modelling the measurement actions can be seen in 8. Although this limits the range of planners that can solve problems in our domain, a simplified domain (where the `sqrt` function is simply omitted) can also be used on all of the problem files.

Experimental Analysis

The experiments were performed on a AMD Phenom II 3.50 GHZ processor with 4 GB of RAM. A modified version of LPG-td (Gerevini, Saetti, & Serina 2008) (to allow for longer formulae, and the square root function) was used in the experiments. The results show the most efficient plan was produced within a 10 minute CPU time limit. All the produced plans are then validated using VAL (Howey,


```

(at start (assign (start-temp) (temp)))
(at start (assign (temp-u)
  ;calculate udevice using the length to measure. (Equation 1)
  (+(*(/(* (u calib ?in) (length-to-measure ?ax ?er)) (k value ?in))
    (/(* (u calib ?in) (length-to-measure ?ax ?er)) (k value ?in)))
  (+(*(/(* (u calib ?in) (length-to-measure ?ax ?er)) (k value ?in))
    (/(* (u calib ?in) (length-to-measure ?ax ?er)) (k value ?in)))
  ;calculate umisalignment. (Equation 3)
  (+(*(/(+ (umisalignment ?in) (umisalignment ?in)) (2sqr3))
    (/(+ (umisalignment ?in) (umisalignment ?in)) (2sqr3)))
  ;calculate uerror interrelated contributors.
  (+(*(/(+ (error-val ?ax ?e1) (error-val ?ax ?e2)) (2sqr3))
    (/(+ (error-val ?ax ?e1) (error-val ?ax ?e2)) (2sqr3)))
  ;calculate ummachine tool. (Equation 4)
  (+(*(* (ut-m-d) (* (length-to-measure ?ax ?er) (u-m-d)))
    (* (ut-m-d) (* (length-to-measure ?ax ?er) (u-m-d))))
  ;calculate umdevice. (Equation 6)
  (+(*(* (ut-m-d) (* (length-to-measure ?ax ?er) (u-m-d)))
    (* (ut-m-d) (* (length-to-measure ?ax ?er) (u-m-d))))
  ;calculate ueve. (Equation 8)
  (*(/ (ueve) (2sqr3)) (/ (ueve) (2sqr3))))))
)
(at end
  (increase (u-c) (sqrt
    (+ (temp-u)
      (* (* (ut-e-c) (* (length-to-measure ?ax ?er) (- (temp) (start-temp))))
      (* (ut-e-c) (* (length-to-measure ?ax ?er) (- (temp) (start-temp))))))))

```

Figure 8: Partial PDDL code showing part of the measure-influence action.

Long, & Fox 2004). These experiments were carried out without the ability to schedule measurements concurrently. The experimental evidence suggests that a temporally optimised plan is not necessarily a plan which has a small uncertainty of measurement. The reverse is also true: plans with a small uncertainty of measurement are not necessary ones with short makespans.

To examine this relationship between optimisation of temporal and the uncertainty of measurement, twelve different problem instances are used and optimised for following three different metrics:

1. U - (:metric minimize (u-m))
2. T - (:metric minimize (total-time))
3. $\frac{U+T}{2}$ - (:metric minimize (/ (+ (u-c) (totaltime)) 2))

Table 1 shows the empirical data from performing these experiments. From these results, it is evident that when optimising for time, no consideration is taken to the uncertainty due to the plan order. Similarly, it is evident that when optimising for the uncertainty due to the plan order, no consideration to temporal implications is taken. However, when optimising the plan to both the uncertainty due to the order of the plan and to reduce the overall timespan, it is evident that the planner can establish a good compromise.

Plan Excerpt

The plan excerpt shown in Figure 9 shows the plan order when optimising both machine tool downtime and the uncertainty of measurement due to the plan order for problem instance 3A1A. Firstly, it is evident that temporal optimisation has been achieved by scheduling measurements that use the same instrumentation sequentially so that the instrumentation only needs to be adjusted, not removed and set-up once again. Secondly, it can be seen that the uncertainty of mea-

Instance	Optimise T		Optimise U		Optimise T & U	
	T	U(μm)	T	U(μm)	T	U(μm)
3A1A	33:12	200	34:12	18	33:38	27
3A1B	29:42	150	28:03	138	30:12	138
3A1C	29:21	199	31:45	193	29:21	193
3A2A	31:14	93	33:00	27	31:19	33
3A2B	28:27	90	30:34	82	28:57	82
3A2C	26:04	152	27:05	93	26:05	116
5A1A	52:05	99	56:56	52	55:11	53
5A1B	52:28	76	55:11	55	52:55	72
5A1C	50:18	66	51:29	59	50:54	70
5A2A	47:46	142	50:58	92	50:28	115
5A2B	45:17	135	47:46	94	46:05	112
5A2C	47:46	211	49:11	142	48:27	168

Table 1: Temporal & Uncertainty optimisation result

E_{YX} : Straightness in the Y-Axis direction
 E_{ZX} : Straightness in the Z-Axis direction
 E_{ZY} : Straightness in the Z-Axis direction
 E_{XY} : Straightness in the X-Axis direction
 E_{XZ} : Straightness in the X-Axis direction
 E_{YZ} : Straightness in the Y-Axis direction
 E_{COY} : Non-orthogonality between the Y- and X-axis
 E_{COZ} : Non-orthogonality between the Z- and Y-axis
 E_{COY} : Non-orthogonality between the X- and Z-axis

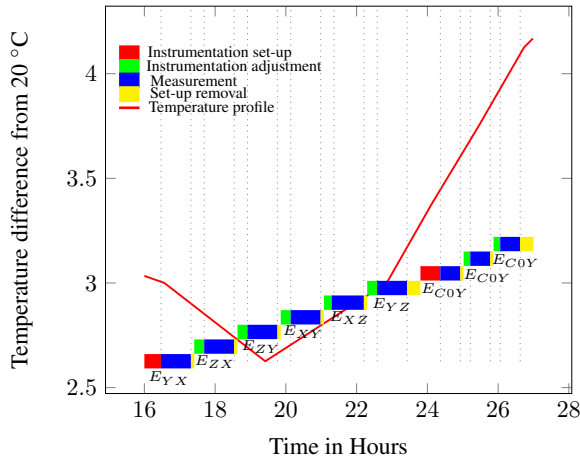


Figure 9: Uncertainty and Temporal Optimisation.

surement due to the plan order has been reduced by scheduling interrelated measurements together as well as scheduling them where the temperature difference is at its lowest.

From examining the temperature profile seen in Figure 5, it is evident that there are areas where the temperature difference is lower. However, when solving multi-optimisation planning problems, a trade-off between both metrics is going to take place. In Table 1, this trade-off can be seen where the calibration plan duration is 33 hours 38 minutes and the uncertainty of measurement metric is 37.33 μm . It is evident that both metrics are not as low as when optimising for them individually, but it is clear that the plan is a good compromise showing significant reduction in both machine tool downtime and the uncertainty of measurement due to the plan order. In comparison between optimum plans, the metrics in the multi-objective plans on average 1.68% worse for time and 17% worse for the uncertainty of measurement than when they are optimised individually. However, the multi-object search plans are on average have a 2.69% reduction in the time metric when compared to the downtime of the uncertainty optimised plan and a 18.5% improvement in estimated uncertainty of measurement metric when compared to the uncertainty of the temporally optimised plan.

Future Work

This paper presents machine tool calibration as example of where the reduction in the uncertainty of measurement has significant implications. However, the presented work provides a significant contribution to the metrology community, showing how the use of automated planning can optimise

calibration plans to reduce the uncertainty of measurement. Currently, the uncertainty of measurement is estimated for individual measurements in metrology, and even though the effects of interrelated errors are known, the associated complexity means that little consideration is taken to producing an optimal sequence of measurements that can reduce the uncertainty of measurement. The work presented in this paper increases the state-of-the-art in calibration planning and uncertainty estimation, and will be deployed to calibration engineers in the field in a decision support tool.

Conclusions

Creating a calibration plan by hand, that minimises machine tool downtime and measurement uncertainty, is a difficult and time-consuming activity. Balancing the reduction in uncertainty with the resulting increase in time required only makes the task harder. Any software tool that can assist in this activity can save engineers time in creating and executing the calibration plan, and can save the client time in reduced machine downtime. Now, due to our new model, the client can also be guaranteed a more accurate result.

This work demonstrates that by extending our previously created machine tool calibration domain model, not only can machine tool downtime be reduced, but so can the uncertainty of measurement. Encoding the relevant domain knowledge resulted in the discretization of the continuous temperature profile that is then encoded by stitching durative actions together. In creating the model we have developed a robust preprocessor that provides a square root function that can be used in a generic PDDL domain to specified levels of relative error.

Experimental data has shown that the model performs well when optimising for both metrics to reduce the makespan and the accumulated uncertainty of measurement numeric fluent. On average, when trying to optimise both metrics together, there is an increase of downtime and the uncertainty of measurement of 9%. However, the experimental analysis displays that this is not too detrimental, resulting in the observation that performing a multi-objective search is feasible. The multi-optimisation metric considered in this paper considers an equal weighting between time and uncertainty. However, it can be easily expanded to add weighting so that the client can weight one metric in favour the other.

Acknowledgement

The authors gratefully acknowledge the UK's Engineering and Physical Science Research Council (EPSRC) funding of the EPSRC Centre for Innovative Manufacturing in Advance Metrology (Grant Ref: EP/I033424/1).

References

- Bell, S. 2001. A beginner's guide to uncertainty of measurement. *Measurement Good Practice Guide* (11).
- BIPM. 2008. Evaluation of measurement data guide to the expression of uncertainty in measurement.
- Birch, K. 2003. Estimating uncertainties in testing. *Measurement Good Practice Guide* (36).

- Forbes, A. 2006. Measurement uncertainty and optimized conformance assessment. *Measurement* 39(9):808 – 814.
- Fox, M., and Long, D. 2003. Pddl2.1: An extension to pddl for expressing temporal planning domains. *Journal of Artificial Intelligence Research (JAIR)* 20:61–124.
- Fox, M.; Long, D.; and Halsey, K. 2004. An investigation into the expressive power of PDDL 2.1. In *ECAI*, volume 16, 338.
- Gerevini, A.; Saetti, A.; and Serina, I. 2006. An Approach to Temporal Planning and Scheduling in Domains with Predictable Exogenous Events. *Journal of Artificial Intelligence Research (JAIR)* 25:187–231.
- Gerevini, A. E.; Saetti, A.; and Serina, I. 2008. An approach to efficient planning with numerical fluents and multi-criteria plan quality. *Artificial Intelligence* 172(8):899–944.
- Howey, R.; Long, D.; and Fox, M. 2004. Val: Automatic plan validation, continuous effects and mixed initiative planning using pddl. In *Tools with Artificial Intelligence, 2004. ICTAI 2004. 16th IEEE International Conference on*, 294–301. IEEE.
- ISO 230-2. 2006. *Test code for machine tools – Part 2: Determination of accuracy and repeatability of positioning numerically controlled axes*. ISO, Geneva, Switzerland.
- ISO 230-9. 2005. *Test code for machine tools – Part 9: Estimation of measurement uncertainty for machine tool tests according to series ISO 230, basic equations*. International Standards Organisation.
- ISO230. 2012. *Part 1: Geometric accuracy of machines operating under no-load or quasi-static conditions*. International Standards Organisation.
- Long, D., and Fox, M. 2003. The 3rd International Planning Competition: Results and analysis. *Journal of Artificial Intelligence Research (JAIR)* 20:1–59.
- Parkinson, S.; Longstaff, A.; Fletcher, S.; Crampton, A.; and Gregory, P. 2012a. Automatic planning for machine tool calibration: A case study. *Expert Systems with Applications* 39(13):11367 – 11377.
- Parkinson, S.; Longstaff, A. P.; Crampton, A.; and Gregory, P. 2012b. The application of automated planning to machine tool calibration. In McCluskey, T.; Williams, B.; Silva, J. R.; and Bonet, B., eds., *Proceedings of the Twenty-Second International Conference on Automated Planning and Scheduling*, ICAPS 2012. California, USA: AAAI Press. 216–224.
- Schwenke, H.; Knapp, W.; Haitjema, H.; Weckenmann, A.; Schmitt, R.; and Delbressine, F. 2008. Geometric error measurement and compensation of machines - an update. *CIRP Annals-Manufacturing Technology* 57(2):660–675.
- Shagluf, A.; Longstaff, A.; and Fletcher, S. 2013. Towards a downtime cost function to optimise machine tool calibration schedules. In *Proceedings of the International Conference on Advanced Manufacturing Engineering and Technologies NEWTECH 2013*, volume 16, 231–240. KTH Royal Institute of Technology, Stockholm, Sweden.